PHYSICAL REVIEW D **88,** 055015 (2013)

Peccei-Quinn symmetry as the origin of Dirac neutrino masses

Chian-Shu Chen[1,3,*] and Lu-Hsing Tsai[2,†]

[1] *Physics Division, National Center for Theoretical Sciences, Hsinchu, Taiwan 300*
[2] *Department of Physics, National Tsing Hua University, Hsinchu, Taiwan 300*
[3] *Institute of Physics, Academia Sinica, Taipei, Taiwan 115*
(Received 8 March 2013; published 17 September 2013)

We propose a model of Dirac neutrino masses generated at one-loop level. The origin of this mass is induced from Peccei-Quinn symmetry breaking which was proposed to solve the so-called strong *CP* problem in QCD; therefore, the neutrino mass is connected with the QCD scale, Λ_{QCD}. We also study the parameter space of this model, confronting neutrino oscillation data and leptonic rare decays. The phenomenological implications to leptonic flavor physics, such as the electromagnetic moment of charged leptons and neutrinos, are studied. Axion as the dark matter candidate is one of the byproducts in our scenario. Diphoton and Z-photon decay channels in the LHC Higgs search are investigated. We show that the effects of a singly charged singlet scalar can be distinguished from the general two Higgs doublet model.

DOI: 10.1103/PhysRevD.88.055015 PACS numbers: 14.60.Pq, 12.60.−i, 14.80.−j

I. INTRODUCTION

Small quantities arising in physics usually require the use of new symmetries for explanations [1]. A good example of these is the Peccei-Quinn (PQ) symmetry that plays the role of the solution of the strong *CP* problem [2,3], in which a θ angle appears in the QCD Lagrangian, $\mathcal{L}_{\text{QCD}} \in \theta \frac{g_S^2}{32\pi^2} G^a_{\mu\nu}\tilde{G}^{a\mu\nu}$, and *CP* is violated [4–6].[1] The instanton solution to the gluon field equations satisfies $n = \frac{1}{32\pi^2}\int d^4x G^a_{\mu\nu}\tilde{G}^{a\mu\nu}$ with n's being integers and representing topological charges [7]. The QCD vacuum state hence can be parametrized as $|\theta\rangle = \sum_{n=-\infty}^{n=\infty} e^{in\theta}|n\rangle$, where θ is periodic with period 2π. Furthermore, for nonzero quark masses the chiral anomaly relates the weak phase in quark masses to the QCD θ term. One can parametrize the θ angle as $\bar{\theta} = \theta - \arg\{\det m_q\}$ [8,9]. It induces a neutron electric dipole moment (EDM) [10–14], and the current experimental upper bound sets the best constraint on $\bar{\theta}$ to be smaller than 0.6×10^{-10} [15]. This extremely suppressed quantity is called the strong *CP* problem. The Peccei-Quinn solution to the strong *CP* problem postulates a global chiral $U(1)_{PQ}$ symmetry and makes $\bar{\theta}$ a dynamical variable, and the shift symmetry of the Nambu-Goldstone boson, axion, corresponding to $U(1)_{PQ}$ [16,17] will set $\bar{\theta}$ zero at classical potential [18]. At one-loop level the chiral anomaly will break the shift symmetry. As a result the axion is not massless but requires a small mass $m_a \simeq \frac{\sqrt{m_u m_d}}{(m_u+m_d)}\frac{f_\pi m_\pi}{f_a} \sim \frac{\Lambda^2_{\text{QCD}}}{f_a}$ [19–21]. Here f_a is the $U(1)_{PQ}$ breaking scale and f_π is the pion decay constant. The laboratory [22] and outer space [23–27] searches have set 10^9 GeV $\lesssim f_a \lesssim 3 \times 10^{11}$ GeV as the allowed regions; therefore, the axion window is 3×10^{-3} eV $> m_a > 10^{-6}$ eV.

On the other hand, another small quantity that puzzles high energy physicists is the masses of neutrinos measured from neutrino oscillation experiments [22]. The key point to understand neutrino physics lies on whether the neutrinos are Dirac fermions or Majorana fermions. This ambiguity comes from the fact that zero electric charge is carried by neutrinos. The tiny neutrino masses may be explained in terms of lepton number (L) symmetry, which is a global $U(1)$ quantum number tagged on lepton sectors in the standard model (SM). If $U(1)_L$ is broken, one can write the dimension-5 Weinberg operator to generate neutrino masses $m_\nu \propto \frac{HHLL}{\Lambda_L}$ [28], where H and L are the SM Higgs and the left-handed lepton fields, respectively, and Λ_L is the breaking scale of $U(1)_L$. In this case neutrinos are regarded as Majorana fermions. However, the Majorana or Dirac nature of the neutrinos is unknown and is awaiting the experimental determination from some lepton number violating processes such as the neutrinoless double beta decay. It is important to consider the possibility that Dirac neutrino masses may also connect with some global symmetry and how those small quantities we observe in physics are related to each other.[2] In this paper we propose a simple Dirac neutrino mass model which is generated by PQ symmetry breaking, and hence the neutrino masses are closely related with axion mass.[3]

*chianshu@phys.sinica.edu.tw
†lhtsai@phys.nthu.edu.tw

[1] The $G^a_{\mu\nu}$ are the $SU(3)_C$ gauge fields with $a = 1, 2, \ldots, 8$ and $\tilde{G}^{a\mu\nu} = \frac{1}{2}\epsilon^{\mu\nu\alpha\beta}G^a_{\alpha\beta}$.

[2] The interesting models of connecting Dirac neutrino mass with leptogenesis are studied, for example, in Refs. [29–31].

[3] In Ref. [32], the PQ symmetry and Dirac neutrino masses are connected in the so-called universal seesaw model. A similar idea of linking Majorana neutrino masses with PQ symmetry was also studied in Refs. [33–42].

TABLE I. Quantum numbers of $U(1)_{PQ}$ and gauge symmetries for leptons and scalars.

	L_L	l_R	H_1	H_2	ν_{R_i}	s_1^+	s_2^+	a
Y	$-\frac{1}{2}$	-1	$\frac{1}{2}$	$\frac{1}{2}$	0	1	1	0
L	1	1	0	0	1	-2	-2	0
PQ	0	-2	2	-2	0	0	2	-2

This paper is organized as follows: in Sec. II we propose the Dirac mass model which is embedded with PQ symmetry. In Sec. III we consider leptonic rare decays and neutrino oscillation data to investigate the parameter space of the model. Some phenomenological implications for the LHC Higgs search, dark matter, and leptonic flavor physics of this model are discussed in Sec. IV. Then we conclude our results in Sec. V.

II. THE MODEL

Particle content and their quantum numbers in the model are listed in Table I. The Y, L, and PQ represent the hypercharge, lepton number, and $U(1)_{PQ}$ charge, respectively.[4] Two Higgs doublets are introduced because of the existence of the PQ symmetry, and one needs two independent chiral transformations for the up-type and down-type fermions; that is, one scalar doublet H_1 couples to d_R and l_R, while the other one H_2 only couples to u_R by setting opposite PQ charges to doublet scalars. We consider the scenario that neutrinos are Dirac fermions, with three right-handed neutrinos $\nu_{R_i}(i = 1\text{–}3)$ assigned to our model, and hence the theory is lepton number conserved. s_1^+ and s_2^+ are $SU(2)_L$-singlet charged scalars, and a is the axion field which is the Nambu-Goldstone boson of the spontaneously broken $U(1)_{PQ}$. Notice that ν_R's are completely neutral under gauge symmetries and PQ symmetry and only carry the L quantum number. The Dirac neutrino mass term is forbidden by the PQ symmetry at the tree level and is generated at one-loop level after the PQ symmetry breaking by utilizing the charged scalars s_1^+ and s_2^+. The new Yukawa interactions of the model for leptons are given by

$$\mathcal{L} = y_{\alpha\beta}\overline{(L_{L_\alpha})}l_{R_\beta}H_1 + f_{\alpha\beta}\overline{L^c_{L_\alpha}}i\sigma_2(L_{L_\beta})s_1^+ + h_{\alpha i}\overline{l^c_{R_\alpha}}\nu_{R_i}s_2^+ + \text{H.c.}, \tag{1}$$

where c denotes charged conjugation, α, $\beta = e$, μ, τ, and $\sigma_i(i = 1\text{–}3)$ are the Pauli matrices. In general, y and h are complex matrices, and f is an antisymmetric matrix due to the Fermi statistics. One can choose the basis of leptonic mass eigenstates L_L, l_R such that y is a diagonalized matrix. Also f_{ij} can be chosen to be real by rephasing L_L and by transferring the phases into l_R. Therefore, only h_{ij} are complex. The scalar potential can be written as

$$\begin{aligned} V = &-\mu_1^2H_1^\dagger H_1 - \mu_2^2H_2^\dagger H_2 - \mu_a^2|a|^2 + \mu_{s1}^2|s_1|^2 + \mu_{s2}^2|s_2|^2 + \lambda_1(H_1^\dagger H_1)(H_1^\dagger H_1) + \lambda_2(H_2^\dagger H_2)(H_2^\dagger H_2) \\ &+ \lambda_3(H_1^\dagger H_1)(H_2^\dagger H_2) + \lambda_4(H_1^\dagger H_2)(H_2^\dagger H_1) + (H_1^\dagger H_1)[d_1|s_1|^2 + d_2|s_2|^2 + d_a|a|^2)] \\ &+ (H_2^\dagger H_2)[g_1|s_1|^2 + g_2|s_2|^2 + g_a|a|^2] + h_1|s_1|^4 + h_2|s_2|^4 + h_3|s_1|^2|s_2|^2 + h_a|a|^4 + |a|^2(h_{a1}|s_1|^2 + h_{a2}|s_2|^2) \\ &+ [h_5(H_2^\dagger H_1)a^2 + \mu s_1^- s_2^+ a + \text{H.c.}]. \end{aligned} \tag{2}$$

All parameters in the potential are real. Though h_5 and μ are in general complex parameters, one can absorb their phases by redefining $(s_1^\dagger s_2)$, $(H_2^\dagger H_1)$, and a, respectively. For the invisible axion, d_a, g_a, h_{a1}, h_{a2}, h_5, μ should be very small to make other scalar masses not too heavy [43–46]. The details about the scalar mass spectrum are in the Appendix.

The leading contribution to the Dirac neutrino mass at one-loop level is shown in Fig. 1 and is given by

$$(M_\nu)_{\alpha i} = -\frac{\mu f_a}{8\pi^2 m_\beta} f_{\alpha\beta}h_{\beta i}I(m_{s1}^2, m_{s2}^2, m_\beta^2), \tag{3}$$

where $I(m_{s1}^2, m_{s2}^2, m_\beta^2)$ is defined as

$$I(m_{s1}^2, m_{s2}^2, m_\beta^2) = \frac{m_\beta^2}{m_{s1}^2 - m_{s2}^2}\left[\frac{m_{s1}^2}{m_{s1}^2 - m_\beta^2}\log\frac{m_{s1}^2}{m_\beta^2} - \frac{m_{s2}^2}{m_{s2}^2 - m_\beta^2}\log\frac{m_{s2}^2}{m_\beta^2}\right]. \tag{4}$$

In the limit of $m_{s1,2} \gg m_k$, the neutrino mass matrix is proportional to the charged lepton mass, as given by

$$\begin{aligned} (M_\nu)_{\alpha i} &= -\frac{1}{8\pi^2}f_{\alpha\beta}h_{\beta i}m_\beta\frac{\mu f_a}{m_{s1}^2 - m_{s2}^2}\log\frac{m_{s1}^2}{m_{s2}^2} \\ &\approx -\frac{1}{8\pi^2}f_{\alpha\beta}h_{\beta i}\frac{\mu m_\beta}{m_a}\frac{\Lambda_{\text{QCD}}^2}{m_{s1}^2 - m_{s2}^2}\log\frac{m_{s1}^2}{m_{s2}^2} \\ &= -Cf_{\alpha\beta}m_\beta h_{\beta i}. \end{aligned} \tag{5}$$

[4]In this paper two additional global symmetries $U(1)_L$ and $U(1)_{PQ}$ are imposed in the model. It turns out that the two symmetries are not independent, such that $U(1)_L$ can be generated accidentally by some particular choice of $U(1)_{PQ}$ charges. One example is to take the PQ charges as H_1:2, H_2: -2, L_L:1, ν_R:4, l_R: -1, a:1, s_1: -2, and s_2: -3. We found it is a generic feature of assigning the large ratios of the PQ charges for some particles in order to bridge the two global symmetries nontrivially.

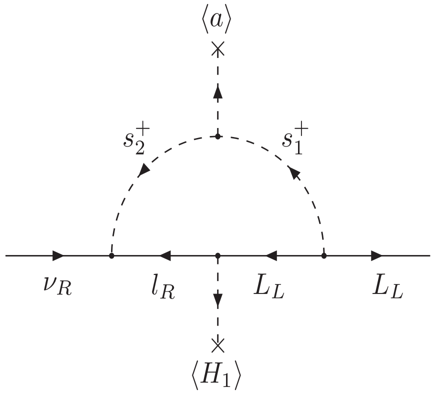

FIG. 1. Induced Dirac neutrino mass.

We have replaced the PQ symmetry breaking scale by the axion mass and the QCD scale in Eq. (5).[5] Note that there are similar constructions discussed in Refs. [48,49]. However, our setup shows the interesting relation between the neutrino Dirac mass and QCD dynamics. Furthermore, the axions can be the dark matter candidate constituting 25% of the energy density in our Universe. From the neutrino mass formula and scalar potential we can see that if one does not tune the couplings h_{a1} and h_{a2}, then the masses of s_1 and s_2 should be of the order of f_a. Combining them with the value of μ to be around the electroweak scale would directly lead to a small quantity of $C \approx 10^{-8}$, which means one can have the observed light neutrino masses with the Yukawa couplings f, h at the order of 10^{-1}. Although such a scenario can naturally provide a tiny neutrino mass without fine-tuning the couplings, in what follows we still focus on the case in which both m_{s1} and m_{s2} are of the electroweak scale to provide richer phenomenological implications. In this case we can see that the large value of f_a lifts up the mass scale of Dirac neutrino masses and in order to keep the smallness of M_ν a combination of suppressed factors will be needed such as the loop factor; the Yukawa couplings f, h; the charged lepton chirality suppression; and the parameter μ. Now we roughly estimate the scale of μ, which is the key parameter controlling the overall mass scale of Dirac neutrino masses, and an investigation of parameter space will be discussed in Sec. III. For $M_\nu \approx 0.1$ eV, $m_{s_{1,2}} \sim \mathcal{O}(100\text{–}1000)$ GeV, and $f_a \approx 10^{12}$ GeV, we have $f \sim 10^{-3}$, $h \sim 10^{-2}$, and $\mu \sim \mathcal{O}(1)$ keV. Let us make two comments on the low scale μ and Dirac neutrino masses: (1) We can explain the small μ by implementing the Froggatt-Nielsen mechanism [50] with PQ symmetry. For example, if we assign the PQ quantum number of a as $\frac{2}{n}$ in Table I, all the terms in the Lagrangian will not change except for the μ coupling in the potential. One can write the effective operator as

$$\frac{1}{\Lambda^{n-2}} s_1^+ s_2^- a^n \xrightarrow[U(1)_{PQ}\text{breaking}]{} \left(\frac{\langle a\rangle}{f_a}\right)^{n-2} \langle a\rangle s_1^+ s_2^- a. \tag{6}$$

Thus, $\mu = (\frac{\langle a\rangle}{f_a})^{n-2}\langle a\rangle$ at low energy scale and can be tuned to a small quantity. Here the PQ symmetry can be broken dynamically by some condensates of a new technicolorlike interaction at high scale [51,52]. This mechanism can also apply to other dimensionless couplings of non-Hermitian terms, such as the h_5 in the potential. (2) The mass scale of Dirac neutrino masses is not necessarily small if neutrinos are Majorana fermions. Although we consider neutrinos as the Dirac fermions, the main concern in this paper is the origin of the Dirac neutrino mass, which in general does not forbid the possibility that neutrinos are the Majorana fermions. Therefore, one can still have heavy right-handed Majorana masses, as inspired by the grand unification theories, and obtain small neutrino masses through a canonical seesaw mechanism. The goal in this paper is to point out that the Dirac neutrino mass is generated by the PQ symmetry breaking.

[5]We should mention that quantum gravity effects do not respect global symmetries [47]; hence, the effective operator of Dirac mass receives an additional contribution suppressed by $\kappa\frac{L\nu^c Ha}{M_{\rm pl}}$, where κ is the coefficient. If one requires that this extra contribution be subdominant, say, less than 10^{-3} eV, κ should be smaller than 10^{-7}.

III. CONFRONTING NEUTRINO OSCILLATION DATA AND LEPTONIC RARE DECAYS

From the standard formalism M_ν can be diagonalized by

$$M_{\nu_{\rm diag}} = V_{\rm PMNS}^\dagger M_\nu V_R^{\nu\dagger} = -V_{\rm PMNS}^\dagger (CfM_{l_{\rm diag}}h)V_R^{\nu\dagger}, \tag{7}$$

where $V_{\rm PMNS}$ is a unitary 3×3 Pontecorvo-Maki-Nakagawa-Sakata (PMNS) matrix and V_R is the transformation matrix for right-handed neutrinos. For convenience we define $FH = V_{\rm PMNS}M_{\nu_{\rm diag}}$ with $H = M_{l_{\rm diag}}(-hV_R^{\nu\dagger})$ and $F = Cf$. Due to the antisymmetric nature of the f matrix, the lightest neutrino is exactly massless in this model. Therefore, we can multiply both sides of the mass matrix by a transformation matrix A to reduce one row in the left-hand side of Eq. (7). One obtains

$$F'H = AV_{\rm PMNS}M_{\nu_{\rm diag}}, \tag{8}$$

where

$$F' = AF = \begin{pmatrix} -F_{e\mu} & 0 & F_{\mu\tau} \\ F_{e\tau} & F_{\mu\tau} & 0 \\ 0 & 0 & 0 \end{pmatrix}, \quad A = \begin{pmatrix} 0 & 1 & 0 \\ 0 & 0 & -1 \\ F_{\mu\tau} & -F_{e\tau} & F_{e\mu} \end{pmatrix}. \tag{9}$$

Then we have

TABLE II. Neutrino oscillation data.

$\sin^2\theta_{12}$	$\sin^2\theta_{23}$	$\sin^2\theta_{13}$	$\Delta m^2_{\rm sun}$	$\Delta m^2_{\rm atm}$
0.30 ± 0.013	$0.41^{+0.037}_{-0.025}$	0.023 ± 0.0023	$(7.50 \pm 0.185) \times 10^{-5}$ eV^2	$(2.47^{+0.069}_{-0.067}) \times 10^{-3}$ eV^2

$$\begin{pmatrix} -F_{e\mu}H_{e1} + F_{\mu\tau}H_{\tau 1} & -F_{e\mu}H_{e2} + F_{\mu\tau}H_{\tau 2} & -F_{e\mu}H_{e3} + F_{\mu\tau}H_{\tau 3} \\ F_{e\tau}H_{e1} + F_{\mu\tau}H_{\mu 1} & F_{e\tau}H_{e2} + F_{\mu\tau}H_{\mu 2} & F_{e\tau}H_{e3} + F_{\mu\tau}H_{\mu 3} \\ 0 & 0 & 0 \end{pmatrix} = \begin{pmatrix} m_{\nu 1}V_{\mu 1} & m_{\nu 2}V_{\mu 2} & m_{\nu 3}V_{\mu 3} \\ -m_{\nu 1}V_{\tau 1} & -m_{\nu 2}V_{\tau 2} & -m_{\nu 3}V_{\tau 3} \\ m_{\nu 1}\sum_l V_{l1}F_l & m_{\nu 2}\sum_l V_{l2}F_l & m_{\nu 3}\sum_l V_{l3}F_l \end{pmatrix}, \quad (10)$$

with $F_l = (F_{\mu\tau}, -F_{e\tau}, F_{e\mu})$.

For the normal hierarchical spectrum with $m_{\nu_1} = 0$, we have the following relations:

$$F_{e\mu} = \frac{V^*_{\tau 1}}{V^*_{e1}} F_{\mu\tau}, \qquad F_{e\tau} = -\frac{V^*_{\mu 1}}{V^*_{e1}} F_{\mu\tau}, \quad (11)$$

and

$$H_{\mu 1} = \frac{V^*_{\mu 1}}{V^*_{e1}} H_{e1}, \qquad H_{\tau 1} = \frac{V^*_{\tau 1}}{V^*_{e1}} H_{e1}. \quad (12)$$

The other terms give $H_{\mu 2}$, $H_{\mu 3}$, $H_{\tau 2}$, $H_{\tau 3}$ in terms of $F_{\mu\tau}$, H_{e2}, and H_{e3}:

$$\begin{aligned} H_{\mu 2} &= \frac{V^*_{\mu 1}}{V^*_{e1}} H_{e2} - \frac{m_{\nu_2}}{F_{\mu\tau}} V_{\tau 2}, \\ H_{\tau 2} &= \frac{V^*_{\tau 1}}{V^*_{e1}} H_{e2} + \frac{m_{\nu_2}}{F_{\mu\tau}} V_{\mu 2}, \\ H_{\mu 3} &= \frac{V^*_{\mu 1}}{V^*_{e1}} H_{e3} - \frac{m_{\nu_3}}{F_{\mu\tau}} V_{\tau 3}, \\ H_{\tau 3} &= \frac{V^*_{\tau 1}}{V^*_{e1}} H_{e3} + \frac{m_{\nu_3}}{F_{\mu\tau}} V_{\mu 3}. \end{aligned} \quad (13)$$

Note that the requirement of a real F matrix make $V_{\rm PMNS}$ include two additional phases besides the ordinary irreducible one. Therefore, the model will not give a conclusive prediction for the Dirac CP phase in the neutrino sector at the current stage.

Similarly for the inverted hierarchical spectrum, $m_{\nu_3} = 0$, we obtain

$$\begin{aligned} &F_{e\mu} = \frac{V^*_{\tau 3}}{V^*_{e3}} F_{\mu\tau}, \qquad F_{e\tau} = -\frac{V^*_{\mu 3}}{V^*_{e3}} F_{\mu\tau}, \\ &H_{\mu 1} = \frac{V^*_{\mu 3}}{V^*_{e3}} H_{e1} - \frac{m_{\nu_1}}{F_{\mu\tau}} V_{\tau 1}, \qquad H_{\tau 1} = \frac{V^*_{\tau 3}}{V^*_{e3}} H_{e1} + \frac{m_{\nu_1}}{F_{\mu\tau}} V_{\mu 1}, \\ &H_{\mu 2} = \frac{V^*_{\mu 3}}{V^*_{e3}} H_{e2} - \frac{m_{\nu_2}}{F_{\mu\tau}} V_{\tau 2}, \qquad H_{\tau 2} = \frac{V^*_{\mu 3}}{V^*_{e3}} H_{e2} + \frac{m_{\nu_2}}{F_{\mu\tau}} V_{\mu 2}, \\ &H_{\mu 3} = \frac{V^*_{\mu 3}}{V^*_{e3}} H_{e3}, \qquad H_{\tau 3} = \frac{V^*_{\tau 3}}{V^*_{e3}} H_{e3}. \end{aligned} \quad (14)$$

We will use the central values of the most recent global fitting of the neutrino oscillation measurements [53] (see Table II) in our analyses. In the meantime the appearance of the new scalars will provide the extra contributions to the lepton flavor violation processes. We investigate the parameter space of the model in terms of the constraints from leptonic rare decays in the following. Before that it is worth mentioning that the size of parameter C is proportional to the factor $\mu f_a/(m^2_{s1} - m^2_{s2}) \log(m^2_{s1}/m^2_{s2})$. If there exists a large hierarchy between m_{s1} and m_{s2}, say, $m_{s2} = k m_{s1}$ with k being a large factor, C is approximately inversely proportional to m^2_{s2}. However, the positive mass eigenvalue condition $m_{s1}m_{s2} > \mu f_a$ will also lead to the result that the upper bound of C is proportional to $1/k$. In general C cannot be too small in order to keep the perturbativity of the Yukawa couplings f and h. So the largest allowed hierarchy between m^2_{s1} and m^2_{s2} is around $k \simeq O(10^3)$. We will also discuss the implication to the parameter space with a hierarchy scenario.

A. $\mu \to e\gamma$

The two relevant Yukawa interactions providing the flavor violations in the charged lepton sector are given by

$$\mathcal{L} = -2 f_{\alpha\beta} \overline{l^c_{L_\alpha}} \nu_{L_\beta} s_1 - h_{\alpha i} \overline{l^c_{R_\alpha}} \nu_{R_i} s_2 + \text{H.c.} \quad (15)$$

Without loss of generality, here ν_{R_i} is the mass eigenstate and we absorb the mixing matrix $-V_R$ into the coupling h. In SM + ν_R the one-loop contribution is constrained stringently by the Glashow-Iliopoulos-Maiani (GIM) mechanism. In this model the main contribution is the one-loop diagrams with photon emission attached to the charged scalars s_1^+ or s_2^+ in the loop. Currently the latest result from the MEG Collaboration gives $B(\mu \to e\gamma) < 2.4 \times 10^{-12}$ [54]. For $l_\alpha \to l_\beta \gamma$ the effective Lagrangian can be generally written in the form

$$\mathcal{L} = -\frac{1}{2} \bar{l}_\beta \sigma_{\mu\nu} (\tilde{A}_R P_R + \tilde{A}_L P_L) l_\alpha F^{\mu\nu}, \quad (16)$$

where $\tilde{A}_{L,R}$ for this model is given by

$$\tilde{A}_R = \frac{(-1)e}{192\pi^2} \left(4 \sum_\gamma f^*_{\beta\gamma} f_{\alpha\gamma}\right) \frac{m_\alpha}{m^2_{s1}} \quad \text{and}$$

$$\tilde{A}_L = \frac{(-1)e}{192\pi^2} \left(\sum_i h^*_{\beta i} h_{\alpha i}\right) \frac{m_\alpha}{m^2_{s2}}. \quad (17)$$

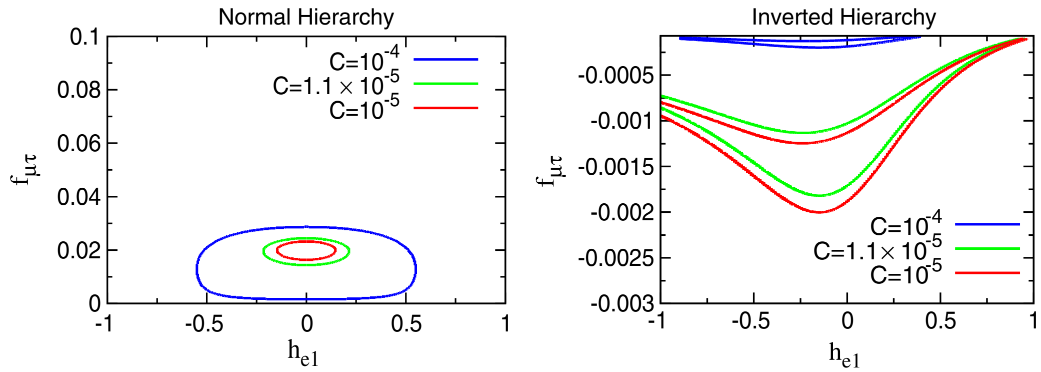

FIG. 2 (color online). The allowed regions in the h_{e1}-$f_{\mu\tau}$ plane in (a) the normal hierarchy and (b) the inverted hierarchy. Different curves are generated with different C (blue: $C = 10^{-4}$, green: $C = 1.1 \times 10^{-5}$, red: $C = 10^{-5}$). The other parameters are taken as $m_{s1} = m_{s2} = 500$ GeV, $h_{e2} = h_{e3} = 0.5$.

Note that the limit $m_\alpha \ll m_{s1,2}$ has been applied to the above formula. The decay rate of $l_\alpha \to l_\beta \gamma$ is $\Gamma(l_\alpha \to l_\beta \gamma) = (m_\alpha^3/16\pi)(1 - m_\beta^2/m_\alpha^2)^3(|\tilde{A}_R|^2 + |\tilde{A}_L|^2)$. One can compare it with the lepton three-body decay width $\Gamma(l_\alpha \to l_\beta \nu_\alpha \bar{\nu}_\beta) = G_F^2 m_\alpha^5/192\pi^3$. The branching ratio $\mu \to e\gamma$ in our model is obtained by

$$\begin{aligned} B(\mu \to e\gamma) &\equiv \frac{\Gamma(\mu \to e\gamma)}{\Gamma(\mu \to e\nu\bar{\nu})} \\ &= \frac{\alpha_e}{768\pi G_F^2} \\ &\quad \times \left(\frac{16 \sum_\gamma |f_{e\gamma}|^2 |f_{\mu\gamma}|^2}{m_{s1}^4} + \frac{\sum_i |h_{ei}|^2 |h_{\mu i}|^2}{m_{s2}^4} \right). \end{aligned} \quad (18)$$

The results are given in Fig. 2. Here we consider that $f_{\mu\tau}$ is positive for the normal hierarchy spectrum and negative for the inverted hierarchy spectrum, respectively. The allowed regions are rather small and sensitive to the value of C. For example, the parameter space will shrink to zero if we take $C = 0.8 \times 10^{-5}$ with the same inputs.

B. μ–e conversion

The one-loop diagrams for μ–e conversion include photon penguin diagrams, Z penguin diagrams, and box diagrams. Again the contribution from the diagrams involving W boson exchange is suppressed by the GIM mechanism, and the leading contributions come from the penguin diagrams with the charged scalars s_1^+ and s_2^+ in the loop. In contrast, the leading Z penguin contribution is suppressed by the light charged scalars. Therefore, only the photon penguin needs to be taken into account. The corresponding effective Lagrangian is given by

$$\begin{aligned} \mathcal{L} = &-\frac{G_F}{\sqrt{2}} \frac{s_W^2}{36\pi^2} m_W^2 \bar{e}\gamma_\mu \Big(\sum_\alpha 4 f_{e\alpha}^* f_{\mu\alpha} \frac{1}{m_{s1}^2} P_L \\ &+ \sum_i h_{ei}^* h_{\mu i} \frac{1}{m_{s2}^2} P_R \Big) \mu \sum_q Q_q \bar{q}\gamma^\mu q. \end{aligned} \quad (19)$$

In the above we used the shorthand notation $s_W \equiv \sin\theta_W$. The μ–e conversion with nucleons in an atom has been calculated in detail in Ref. [55], and we will adopt their notation in what follows. The general interactions associated with μ–e conversion are written as

$$\begin{aligned} \mathcal{L}_{\rm eff} = &-\frac{4G_F e}{\sqrt{2}}[m_\mu \bar{e}\sigma^{\mu\nu}(A_R P_R + A_L P_L)\mu F_{\mu\nu} + \text{H.c.}] - \frac{G_F}{\sqrt{2}}[\bar{e}(g_{LS(q)}P_R + g_{RS(q)}P_L)\mu\bar{q}q + \bar{e}(g_{LP(q)}P_R \\ &+ g_{RP(q)}P_L)\mu\bar{q}\gamma_5 q + \text{H.c.}] - \frac{G_F}{\sqrt{2}}[\bar{e}(g_{LV(q)}\gamma^\mu P_L + g_{RV(q)}\gamma^\mu P_R)\mu\bar{q}\gamma_\mu q + \bar{e}(g_{LA(q)}\gamma^\mu P_L \\ &+ g_{RA(q)}\gamma^\mu P_R)\mu\bar{q}\gamma_\mu\gamma_5 q + \text{H.c.}] - \frac{G_F}{\sqrt{2}}\Big[\frac{1}{2}\bar{e}(g_{LT(q)}\sigma^{\mu\nu}P_R + g_{RT(q)}\sigma^{\mu\nu}P_L)\mu\bar{q}\sigma_{\mu\nu}q + \text{H.c.}\Big], \end{aligned} \quad (20)$$

where $A_{R,L}$ is related to the dipole interaction with photons and $g_{S,P,V,A,T}$ indicate scalar, pseudoscalar, vector, axial vector, and tensor couplings, respectively. Comparing the above formula with Eq. (19), we have

$$g_{LV}^{(q)} = \frac{Q_q s_W^2}{36\pi^2} m_W^2 \Big(\sum_\alpha 4 f_{e\alpha}^* f_{\mu\alpha} \frac{1}{m_{s1}^2} \Big), \qquad g_{RV}^{(q)} = \frac{Q_q s_W^2}{36\pi^2} m_W^2 \Big(\sum_i h_{ei}^* h_{\mu i} \frac{1}{m_{s2}^2} \Big), \quad (21a)$$

$$A_R = \frac{(-1)}{192\pi^2 g_2^2} \Big(\sum_\alpha 4 f_{e\alpha}^* f_{\mu\alpha} \frac{m_W^2}{m_{s1}^2} \Big), \qquad A_L = \frac{(-1)}{192\pi^2 g_2^2} \Big(\sum_i h_{ei}^* h_{\mu i} \frac{m_W^2}{m_{s2}^2} \Big), \quad (21b)$$

and other couplings vanish. The rate of μ–e conversion with nucleons in atom A is usually normalized to the rate of muon capture by A. The conversion-to-capture ratio can be derived in the form

$$B^A_{\mu\to e} = \frac{2G_F^2 m_\mu^5}{\Gamma^A_{\rm capt}}(|eA_R D + \tilde{g}^{(p)}_{LV}V^{(p)} + \tilde{g}^{(n)}_{LV}V^{(n)}|^2 + |eA_L D + \tilde{g}^{(p)}_{RV}V^{(p)} + \tilde{g}^{(n)}_{RV}V^{(n)}|^2) \quad (22)$$

with $\tilde{g}^{(p)}_{L,RV} = 2g^{(u)}_{L,RV} + g^{(d)}_{L,RV}$ and $\tilde{g}^{(n)}_{L,RV} = g^{(u)}_{L,RV} + 2g^{(d)}_{L,RV}$. D and $V^{(p,n)}$ are overlapped functions which can be found in Ref. [55]. The constraints from experimental results for μ–e conversion in different nuclei [56–60] are weaker than what is given by $\mu \to e\gamma$.

C. μ–$3e$

Penguin diagrams and box diagrams contribute to this process. The experimental upper bound is $B(\mu \to e\bar{e}e) < 10^{-12}$ [61]. The contribution of the SM with right-handed neutrino singlets to these processes is suppressed by the neutrino mass. The corresponding one-loop diagrams in this model for $\mu \to 3e$ are similar to those for μ–e conversion, with the quarks replaced by electrons. In general the effective Lagrangian for $\mu \to e\bar{e}e$ is

$$\mathcal{L}(\mu \to e\bar{e}e) = -\frac{4G_F}{\sqrt{2}}\Big[\bar{e}\gamma_\mu e\frac{q_\nu}{q^2}\bar{e}i\sigma^{\mu\nu}(8\pi\alpha_e m_\mu)(A_R P_R + A_L P_L)\mu + \bar{e}\gamma^\mu(a_L P_L + a_R P_R)e\bar{e}\gamma_\mu P_L\mu + \bar{e}\gamma^\mu(b_L P_L + b_R P_R)e\bar{e}\gamma_\mu P_R\mu\Big]. \quad (23)$$

The branching ratio can be calculated as

$$B(\mu \to e\bar{e}e) \simeq (|a_R|^2 + |b_L|^2) + 2(|a_L|^2 + |b_R|^2) - 32\pi\alpha_e\,{\rm Re}(A_R(a_R + 2a_L) + A_L(b_L + 2b_R)) + 256\pi^2\alpha_e^2(|A_R|^2 + |A_L|^2)\Big(4\ln\frac{m_\mu}{m_e} - \frac{11}{2}\Big), \quad (24)$$

where the parameters $a_{L,R}$ and $b_{L,R}$ are given by

$$a_{L,R} = -\frac{s_W^2}{144\pi^2}m_W^2\Big(\sum_\alpha 4f^*_{e\alpha}f_{\mu\alpha}\frac{1}{m_{s1}^2}\Big) \quad \text{and}$$
$$b_{L,R} = -\frac{s_W^2}{144\pi^2}m_W^2\Big(\sum_i h^*_{ei}h_{\mu i}\frac{1}{m_{s2}^2}\Big) \quad (25)$$

from the photon penguin diagrams, while for the box diagrams the leading order of $a_R^{\rm box}$ and $b_L^{\rm box}$ vanishing, we have

$$a_L^{\rm box} = \frac{m_W^2}{32\pi^2 g_2^2 m_{s1}^2}\Big|\sum_\alpha 4f_{\mu\alpha}f^*_{e\alpha}\Big|\Big|\sum_{\alpha'} 4f^*_{e\alpha'}f_{e\alpha'}\Big| \quad (26a)$$

and

$$b_R^{\rm box} = \frac{m_W^2}{32\pi^2 g_2^2 m_{s2}^2}\Big|\sum_i h_{\mu i}h^*_{ei}\Big|\Big|\sum_{i'} h^*_{ei'}h_{ei'}\Big|, \quad (26b)$$

respectively. As shown in Fig. 2, the Yukawa coupling f is in the range of $\mathcal{O}(10^{-2})$ to $\mathcal{O}(10^{-3})$; we can safely ignore the box diagram contributions in $\mu \to 3e$ decay. Therefore, the parameter space is looser than those of $\mu \to e\gamma$.

In the limit of mass hierarchy between m_{s1} and m_{s2}, that is, the $m_{s1} > m_{s2}$ or $m_{s2} > m_{s1}$ cases, the parameter space for Yukawa couplings h and f in both the normal hierarchy and inverted hierarchy neutrino mass spectrum, respectively, are shown in Figs. 3 and 4. Here we take $m_{s1} = 20m_{s2}$ and $m_{s2} = 5m_{s1}$ as the reference points. In these cases, we are only able to give a severe constraint on one of the couplings, h or f, and we illustrate our results by taking a 500 GeV mass scale to the lighter scalar field.

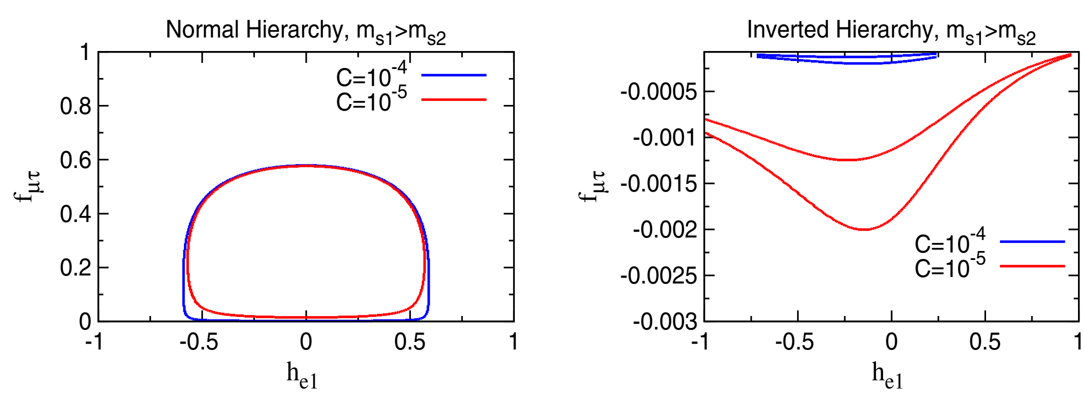

FIG. 3 (color online). The allowed regions in the h_{e1}-$f_{\mu\tau}$ plane for the case of $m_{s1} = 20m_{s2}$ in the normal hierarchy and inverted hierarchy neutrino mass spectrum, respectively. The blue line corresponds to $C = 10^{-4}$ and the red line represents $C = 10^{-5}$.

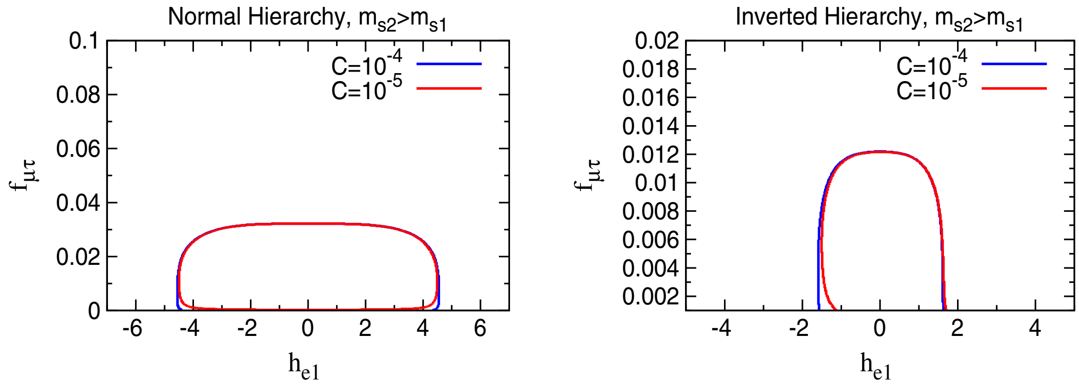

FIG. 4 (color online). The allowed regions in the h_{e1}-$f_{\mu\tau}$ plane for the case of $m_{s2} = 5m_{s1}$ in the normal hierarchy and inverted hierarchy neutrino mass spectrum, respectively. The blue line corresponds to $C = 10^{-4}$ and the red line represents $C = 10^{-5}$.

IV. PHENOMENOLOGY

A. Electromagnetic moments of leptons

1. Muon g − 2

The anomalous magnetic moment of the muon is an observable as a precision test in the SM. The current experimental results [62,63] reported that the muon $g-2$ deviation from the SM prediction is $a_\mu(\mathrm{exp}) - a_\mu(\mathrm{SM}) = (287 \pm 63 \pm 49) \times 10^{-11}$, which indicates some new physics contribution. Our scenario is essentially a two Higgs doublet model (2HDM) plus two singly charged scalars $s_1^\pm$ and $s_2^\pm$. The anomalous $g-2$ of the muon in this model is given by

$$\Delta a_\mu = -\frac{m_\mu^2}{96\pi^2}\Bigg[4\sum_\alpha |f_{\mu\alpha}|^2\frac{1}{m_{s1}^2} + \sum_i |h_{\mu i}|^2\frac{1}{m_{s2}^2} + \frac{m_\mu^2}{v^2}\bigg(\frac{14c_{\beta-\alpha}^2}{m_h^2\cos^2\beta} + \frac{14s_{\beta-\alpha}^2}{m_H^2\cos^2\beta} - \frac{22\tan^2\beta}{m_A^2} + \frac{\tan^2\beta}{m_{H^+}^2}\bigg)\Bigg], \tag{27}$$

where h and H are scalar particles with h being the SM-like Higgs, as well as the pseudoscalar field A and the charged scalars $H^\pm$. α, β are the mixing angles $[s_{\beta-\alpha} \equiv \sin(\beta-\alpha)$ and $c_{\beta-\alpha} \equiv \cos(\beta-\alpha)]$ defined in the usual 2HDM (see, e.g., [64,65] and references within). Comparing this with the current experimental result, our model gives a rather small contribution to Δa_μ but is still within the experimental errors.

2. Magnetic moments of neutrinos

Neutrinos can have magnetic moments when they are massive. The present upper bound of neutrino magnetic moments from experiments is $\mu_\nu < 3.2 \times 10^{-11}\mu_B$ [66]. The ordinary leading order contribution in the SM, including right-handed Dirac neutrinos, is the exchange of W, which is around $(3.2 \times 10^{-19}\mu_B)(m_{\nu_i}/\mathrm{eV})$ [67] with the Bohr magneton $\mu_B \equiv e/2m_e$. In this model, the main new contribution comes from the mixing of $s_{1,2}^+$ in the loop, since the same diagram also generates neutrino masses, given by

$$|\mu_\nu^s| = 2m_i e\left(\log\frac{m_{s2}^2}{m_{s1}^2}\right)^{-1}\left(\frac{1}{m_{s1}^2} - \frac{1}{m_{s2}^2}\right) \approx 10^{-19}\mu_B. \tag{28}$$

Note that it only depends on the neutrino and scalar masses, and this contribution is comparable to that associated with W exchange. It is understandable that without imposing a symmetry [68] or employing a spin suppression mechanism to m_ν [69], the generic size of the Dirac neutrino magnetic moment cannot exceed $10^{-14}\mu_B$ [70]. The contributions from other charged scalars such as H^+, s_1^+, and s_2^+ in the loop are less than $\mathcal{O}(10^{-25})\mu_B$, with the result that they do not contribute to neutrino masses.

3. EDM of leptons

Since there is a physical CP phase between the Yukawa couplings f and h, in general, we have the new contributions to the electric dipole moment of charged leptons. The exchange of singly charged scalars gives the EDM to the charged leptons at one-loop level as

$$d_l = -\frac{e}{(4\pi)^2}\sum_i \mathrm{Im}(2h_{li}^*(fV)_{li})\frac{\mu f_a}{m_{s1}^2 - m_{s2}^2} \times\left[\frac{1}{m_{s1}}B\left(\frac{m_{\nu_i}^2}{m_{s1}^2}\right) - \frac{1}{m_{s2}}B\left(\frac{m_{\nu_i}^2}{m_{s2}^2}\right)\right], \tag{29}$$

with the function $B(x)$ defined by

$$B(x) = \frac{\sqrt{x}}{2(1-x)^2}\left(1 + x + \frac{2x\ln(x)}{1-x}\right). \tag{30}$$

Therefore we conclude that the extra contribution is smaller than $\mathcal{O}(\frac{m_\nu^2}{m_l m_s^2})$, which means $|d_e| \lesssim 10^{-35}e\,\mathrm{cm}$. Similarly, the neutrino EDM generated by $s_{1,2}^+$ mixing in the loop gives $|d_\nu| \lesssim 10^{-26}e\,\mathrm{cm}$. Though the new contributions to d_e and d_ν are nonzero, both of them are unobservably small.

B. Dark matter

It is known that the axion field can be a dark matter candidate, constituting a significant fraction of energy density in our Universe. For the purpose of completion we briefly review some aspects of this scenario in this subsection. The properties of the invisible axion are determined by the breaking scale f_a, where its mass and the interactions are inversely proportional to f_a. Hence, the invisible axion is a very light, very weakly interacted, and very long-lived particle. Axions with mass in the range of 10^{-5}–10^{-6} eV were produced during the QCD phase transition with the average momentum of order of the Hubble expansion rate ($\sim 3 \times 10^{-9}$ eV) at this epoch and, hence, are cold dark matter (CDM). Their number density is provided by

$$\Omega_a \simeq \frac{1}{2}\left(\frac{0.6 \times 10^{-5}\ \mathrm{eV}}{m_a}\right)^{\frac{7}{6}}\left(\frac{0.7}{h}\right)^2, \tag{31}$$

where h is the current Hubble expansion rate in units of $100\ \mathrm{kms}^{-1}\,\mathrm{Mpc}^{-1}$. Here we assume that the ratio of the axion number density to the entropy density is constant since produced, and the contribution from topological defect decay is negligible. Recently it was pointed out that the CDM axions would form a Bose-Einstein condensate due to their gravitational interactions [71]. Furthermore, the rethermalization process is so fast that the lowest energy state of the degenerate axion gas consists of a nonzero angular momentum. As a result, a "caustic ring" structure may form in the inner Galactic halo [72–74]. The feature would make the axion a different dark matter from other CDM candidates, and we refer readers to Refs. [71–74] for details.

C. $h \to \gamma\gamma$

We close our discussion on phenomenology by investigating the LHC Higgs results. Both ATLAS [75] and CMS [76] have announced the discovery of a new boson at a mass of 125 GeV which is consistent with the SM Higgs boson via the combined analyses of the $\gamma\gamma$ and ZZ channels. However, the precise values of both production cross sections and decay branch ratios of the new resonance need to be measured to compare with those predictions from the SM. It was pointed out that the branching ratio of Higgs decay into two photons has excess about 1.56 ± 0.43 and 1.9 ± 0.5 times than the SM prediction in both CMS [76] and ATLAS [75] collaborations' data in 2012. Updated results can be found in [77,78]. Although the deviation is still within the SM expectations at the 2σ level, one may consider whether there are new physics effects (see, e.g., [65,79–88] and references therein) In particular, new scalar particles have been widely treated as possible sources. We study the implications of Higgs to diphoton and Higgs to Z-photon decay channels in our model. For simplicity we just consider one singly charged scalar $s^{\pm}$ and omit the subscript in this subsection. The SM Higgs production cross section is modified by the additional doublet scalar in our scenario [65],

$$\sigma_0 = \frac{G_F \alpha_s^2}{128\sqrt{2}\pi}\left|\frac{1}{2}\left(s_\alpha + \frac{c_\alpha}{\tan\beta}\right)A_{1/2}(\tau_t) + \frac{1}{2}(s_\alpha - c_\alpha \tan\beta)A_{1/2}(\tau_b)\right|^2. \tag{32}$$

Notice that the bottom quark contribution is not negligible due to the enhancement of large $\tan\beta$ and $A_{1/2}(\tau) = 2[\tau + (\tau - 1)f(\tau)]\tau^{-2}$ with $\tau_i = \frac{M_h^2}{4M_i^2}$. The function $f(\tau)$ is defined by

$$f(\tau) = \begin{cases} (\sin^{-1}\sqrt{\tau})^2, & \tau \le 1 \\ -\frac{1}{4}\left[\log\frac{1+\sqrt{1-\tau^{-1}}}{1-\sqrt{1-\tau^{-1}}} - i\pi\right]^2, & \tau > 1. \end{cases} \tag{33}$$

In type-II 2HDM the decay rate of $h \to \gamma\gamma$ is given by

$$\Gamma_{\gamma\gamma} = \frac{G_F \alpha^2 m_h^3}{128\sqrt{2}\pi^3}\left|\left(s_\alpha + \frac{c_\alpha}{\tan\beta}\right)\frac{4}{3}A_{1/2}(\tau_t) + (s_\alpha - c_\alpha\tan\beta)\frac{1}{3}A_{1/2}(\tau_b) + s_\alpha A_1(\tau_W) + \lambda' A_0(\tau_{H^+}) + \lambda A_0(\tau_{s^+})\right|^2, \tag{34}$$

where $A_1(\tau) = -[2\tau^2 + 3\tau + 3(2\tau - 1)f(\tau)]\tau^{-2}$ and $A_0(\tau) = -[\tau - f(\tau)]\tau^{-2}$. The coefficients λ and λ' are defined as $\lambda = v\mu_{Hs^+s^-}/(2m_s^2)$ and $\lambda' = v\mu_{HH^+H^-}/(2m_{H^+}^2)$, where $\mu_{Hs^+s^-}$ and $\mu_{HH^+H^-}$ are the related trilinear couplings in the Higgs potential. One can see that the effects of the doublet scalar charged component H^+ and the singly charged singlet s^+ are indistinguishable. The reason is the lack of knowledge of scalar potential. For the $h \to Z\gamma$ channel, the decay width is written as [89]

$$\Gamma_{Z\gamma} = \frac{G_F^2 m_W^2 \alpha m_h^3}{64\pi^4 c_W^2}(1 - m_Z^2/m_H^2)^3 \times \left|\left(s_\alpha + \frac{c_\alpha}{\tan\beta}\right)\left(\frac{1}{2} - \frac{4}{3}s_W^2\right)A_{1/2}(\eta_t, \kappa_t) + (s_\alpha - c_\alpha\tan\beta)\left(\frac{1}{4} - \frac{1}{3}s_W^2\right)A_{1/2}(\eta_b, \kappa_b) + s_\alpha c_W^2 A_1(\eta_W, \kappa_W) + \left(\frac{1}{2} - s_W^2\right)\lambda' A_0(\eta_{H^+}, \kappa_{H^+}) + (-s_W^2)\lambda A_0(\eta_{s^+}, \kappa_{s^+})\right|^2, \tag{35}$$

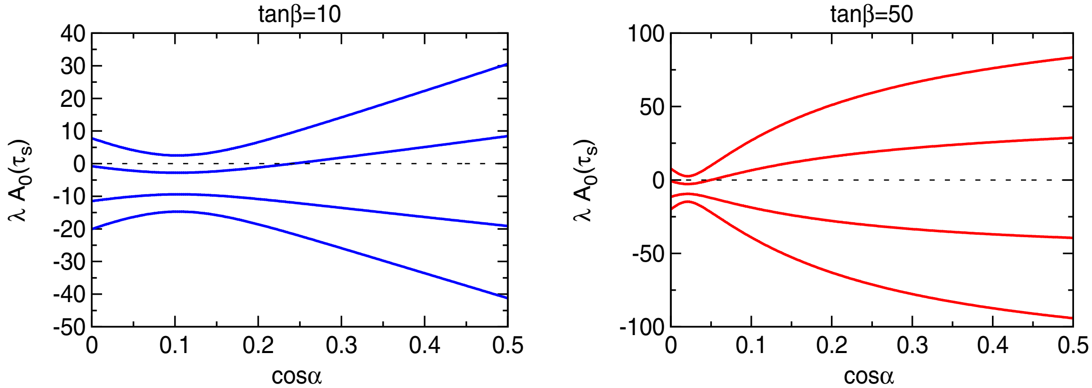

FIG. 5 (color online). Solutions of s^+ effects in terms of $\cos\alpha$ by assuming $A_0(\eta,\kappa)/A_0(\tau) = 1.00$ with $R_{\gamma\gamma} = \frac{\sigma_{\gamma\gamma}}{\sigma_{\gamma\gamma_{\rm SM}}} = 1.5$ and $R_{Z\gamma} = \frac{\sigma_{Z\gamma}}{\sigma_{Z\gamma_{\rm SM}}} = 1$. σ_{ii} and $\sigma_{ii_{\rm SM}}$ are the production cross sections for the Higgs to ii channel in our model and SM, respectively.

where $A_{1/2}(\eta,\kappa) = -4(I_1(\eta,\kappa) - I_2(\eta,\kappa))$, $A_1(\eta,\kappa) = -4(4-\frac{4}{\kappa})I_2(\eta,\kappa) - [(1+\frac{2}{\eta})(\frac{4}{\kappa}-1) - (5+\frac{2}{\eta})]I_1(\eta,\kappa)$, and $A_0(\eta,\kappa) = 2I_1(\eta,\kappa)$, with the parameters $\eta_i = \frac{4M_i^2}{M_h^2}$ and $\kappa_i = \frac{4M_i^2}{M_Z^2}$. Functions $I_1(\eta,\kappa)$ and $I_2(\eta,\kappa)$ are given as

$$I_1(\eta,\kappa) = \frac{\eta\kappa}{2(\eta-\kappa)} + \frac{\eta^2\kappa^2}{2(\eta-\kappa)^2}[f(\eta^{-1}) - f(\kappa^{-1})] + \frac{\eta^2\kappa}{(\eta-\kappa)^2}[g(\eta^{-1}) - g(\kappa^{-1})] \tag{36}$$

and

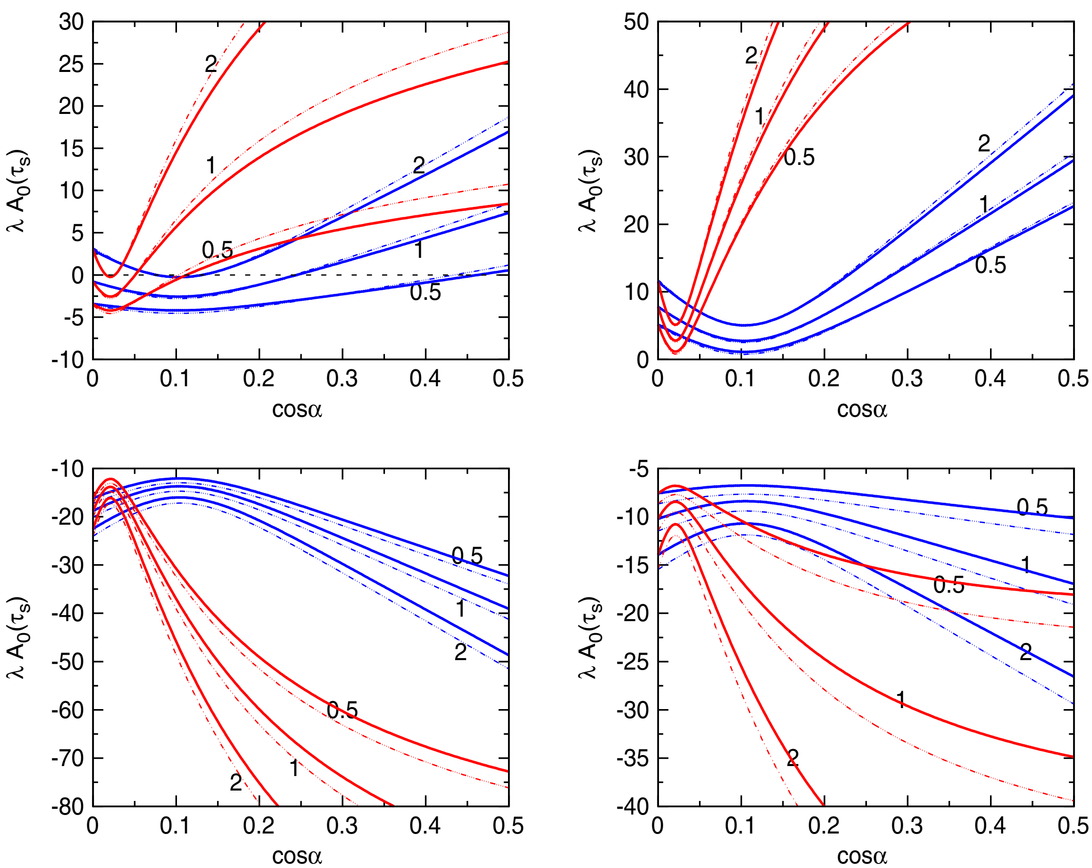

FIG. 6 (color online). Effects of the singly charged singlet scalar with values of $R_{Z\gamma} = 0.5$, 1, 2 as indicated on each curve, and $A_0(\eta,\kappa)/A_0(\tau) = 1.07$ (solid lines), 1.00 (dashed lines), respectively, for the fixed value $R_{\gamma\gamma} = 1.5$. Blue lines correspond to $\tan\beta = 10$ and red lines represent $\tan\beta = 50$. Note that each figure corresponds to one of the lines exhibited in Fig. 5.

$$I_2(\eta, \kappa) = -\frac{\eta\kappa}{2(\eta - \kappa)}[f(\eta^{-1}) - f(\kappa^{-1})], \quad (37)$$

with

$$g(x) = \begin{cases} \sqrt{x^{-1} - 1}(\sin^{-1}\sqrt{x}), & x \leq 1 \\ \frac{\sqrt{1-x^{-1}}}{2}\left[\log\frac{1+\sqrt{1-x^{-1}}}{1-\sqrt{1-x^{-1}}} - i\pi\right], & x > 1 \end{cases}. \quad (38)$$

respectively. Again we see from Eq. (35) that the singly charged singlet effect is hidden in the 2HDM. In order to extract the information of s^+ from the decays, we found the ratio of $A_0(\eta, \kappa)/A_0(\tau)$ lies in the range of 1.00–1.07 with charged scalar masses above 100 GeV. We then take the ratio as a constant and subtract the H^+ contributions in $\Gamma_{\gamma\gamma}$ and $\Gamma_{Z\gamma}$. Other SM Higgs decaying channels are calculated from HDECAY [90]. The results of the s^+ effects in terms of the parameter $\cos\alpha$ with $\tan\beta = 10$, 50 are shown in Fig. 5. Here we take the values $R_{\gamma\gamma} = \frac{\sigma_{\gamma\gamma}}{\sigma_{\gamma\gamma_{SM}}} = 1.5$ and $R_{Z\gamma} = \frac{\sigma_{Z\gamma}}{\sigma_{Z\gamma_{SM}}} = 1$, with σ_{ii} and $\sigma_{ii_{SM}}$ being the production cross sections for the Higgs-to-ii channel in our model and the SM, respectively. Since the new physics effects can have both constructive and destructive interferences with the SM $W^\pm W^\pm$ amplitude, four lines exist in Fig. 5. The results of s^+ effects with different values of $R_{Z\gamma}$ and the ratio of $A_0(\eta, \kappa)/A_0(\tau)$ for the fixed $R_{\gamma\gamma} = 1.5$ are shown in Fig. 6. Here $R_{Z\gamma} = 0.5$, 1, 2 and the $A_0(\eta, \kappa)/A_0(\tau)$ ratios are taken to be 1.07 and 1.00, respectively. It shows that taking the ratio of $A_0(\eta, \kappa)/A_0(\tau)$ as a constant is a good approximation in the regions of parameters we are interested in and is useful for the deviation of $\Gamma_{Z\gamma}$ from the SM prediction for the singly charged singlet scalar s^+. Finally, it is worthwhile to note that the charged singlets s_1^+ and s_2^+ can be produced by quark annihilation through gauge boson γ and Z^0 mediating. This process could have the final states, including two charged leptons, the same as that of $pp \to h \to WW^*$, for which final states of e or μ are tagged by LHC. The related signal strength observed from ATLAS is 1.3 ± 0.5 [91], and the 1σ deviation of it corresponds to around 20 pb. This deviation can be regarded as the allowed space for a new contribution beyond SM. The singly charged scalar production cross section with a parton distribution function given by CTEQ6 [92] is also around 20 pb. with $m_s \simeq 150$ GeV, which can be regarded as the lower bounds on m_s if we assume $\mathrm{Br}(s \to e(\mu)\nu) \simeq 100\%$. Finally, we estimate the background contribution for the $h \to WW^* \to e\nu\mu\nu$ channel from $s^\pm s^\mp$ production. Both singly charged scalars are off shell, and we found that the partial decay width for the center of mass in one of the virtual scalars to be around m_W is negligible compared to the SM prediction.

V. DISCUSSIONS AND CONCLUSIONS

We investigate a model in which neutrinos are Dirac fermions and their masses are generated from the Peccei-Quinn symmetry breaking at one-loop level. As a result, the neutrino mass is related to Λ_{QCD} and the axion appears to be a good candidate for dark matter in explaining the missing energy density of our Universe. Leptonic rare decays constrain the model parameters severely, and therefore, the model can be tested in the near future. We also study the implications of the new scalars to the electromagnetic moments of leptons and recent Higgs signals at LHC, specifically the $h \to \gamma\gamma$ and $h \to Z\gamma$ decays. Finally we would like to make a brief comment on the Majorana extension of our scenario. Lepton number symmetry is one of the keys to understand the underlying neutrino physics. The smoking gun signals to resolve the question are $0\nu\beta\beta$ decays and some lepton number violating processes at LHC. Without direct observations, Majorana neutrinos and Dirac neutrinos are equally good in many aspects at describing phenomena such as neutrino oscillations, leptogenesis, big bang nucleosynthesis, etc. Although we discuss the Dirac neutrino in this model and argue that the Dirac neutrino mass is originated from the Peccei-Quinn symmetry breaking, which is well motivated in QCD field theory, Majorana masses of the right-handed neutrinos, in general, can be formed without violating any principle except the lepton number symmetry. The main modifications are to include some terms in the scalar potential, such as $H_1 H_2 s_1^+$ and $H_1 H_2 a s_2^+$. Therefore, our discussions can be easily embedded in the scenario of Majorana neutrinos where we diagonalize the neutrino mass matrix via the seesaw mechanism.

ACKNOWLEDGMENTS

C.-S. C. is supported by the National Center for Theoretical Sciences, Taiwan, R.O.C., and L.-H. T. is supported by the National Tsing-Hua University (Grant No. 101N1087E1), Taiwan, R.O.C.

APPENDIX: SCALAR MASS SPECTRUM

We briefly analyze the scalar potential given in Eq. (2) and their particle spectrum in this appendix. If the neural components of $H_1 = (h_1^+, (R_1 + iA_1)/\sqrt{2})^T$, $H_2 = (h_2^+, (R_2 + iA_2)/\sqrt{2})^T$ and $a = (R_a + iA_a)/\sqrt{2}$ acquire the vacuum expectation values (VEVs) v_1, v_2, and v_a, respectively, then the related tadpole conditions can be expressed as

$$-\mu_1^2 = -\left[\lambda_1 v_1^2 + \frac{1}{2}(\lambda_3 + \lambda_4)v_2^2 + \frac{1}{2}\left(d_a + h_5\frac{v_2}{v_1}\right)v_a^2\right],$$
$$-\mu_2^2 = -\left[\lambda_2 v_2^2 + \frac{1}{2}(\lambda_3 + \lambda_4)v_1^2 + \frac{1}{2}\left(g_a + h_5\frac{v_1}{v_2}\right)v_a^2\right], \quad (A1)$$

$$-\mu_a^2 = -\left[h_a v_a^2 + h_5 v_1 v_2 + \frac{1}{2}(d_a v_1^2 + g_a v_2^2)\right]. \quad (A2)$$

$v_{1,2}$ are responsible for the electroweak symmetry breaking and $v_a \approx 10^{12}$ GeV is aimed at for the PQ symmetry breaking scale. Notice that the sizes of μ_1, μ_2, and μ_a are not required to be in electroweak scale, while the TeV-scale charged singlets $s_{1,2}$ will bound the couplings $h_{a1,a2}$ to be around v^2/v_a^2 and the value of μ to be less than $(10^3\ \mathrm{GeV})^2/v_a$. Furthermore, the trilinear couplings d_a and g_a for the scalar fields and the axion will be constrained to be larger than v/v_a. The 3×3 scalar neutral mass matrix elements M_{ij} in the basis $\{R_1, R_2, R_a\}$ are given as

$$M_{11}^2 = 2\lambda_1(\cos\beta)^2 v^2 - \frac{h_5}{2}\tan\beta v_a^2, \tag{A3}$$

$$M_{22}^2 = 2\lambda_2(\sin\beta)^2 v^2 - \frac{h_5}{2}\cot\beta v_a^2, \tag{A4}$$

$$M_{33}^2 = 2h_a v_a^2, \tag{A5}$$

$$M_{12}^2 = \frac{1}{2}[(\lambda_3+\lambda_4)(\sin 2\beta)v^2 + h_5 v_a^2], \tag{A6}$$

$$M_{23}^2 = (g_a\sin\beta + h_5\cos\beta)v v_a, \tag{A7}$$

$$M_{13}^2 = (f_a\cos\beta + h_5\sin\beta)v v_a. \tag{A8}$$

The relations $\tan\beta = v_2/v_1$ and $v = (v_1^2+v_2^2)^{1/2}$ are used in the formulas. The mixing angle between $R_{1,2}$ and mass eigenstates H, H_h is defined as $\tan(\beta-\alpha)$, the same as the definition in [65]. The discovery of a 126 GeV scalar implies that the magnitude of h_5 should be of the order v^2/v_a^2. Similarly, the masses of pseudoscalar and charged Higgs bosons are given by

$$m_A^2 = -h_5\left(\sin 2\beta v^2 + \frac{1}{\sin 2\beta}v_a^2\right),$$
$$m_{H^\pm}^2 = -\frac{\lambda_4}{2}v^2 - h_5\frac{1}{\sin 2\beta}v_a^2. \tag{A9}$$

From the above mass formulas we get $h_5 < 0$, and $m_A^2 - m_{H^\pm}^2 = (\lambda_4/2)v^2$ by applying $v_a \gg v$. Finally, the charged particles s_1 and s_2 will not mix with $H^\pm$. The mass matrix elements M_{sij} are given by

$$M_{s11}^2 = \mu_{s1}^2 + h_{a1}v_a^2 + \frac{1}{2}[f_1(\cos\beta)^2 + g_1(\sin\beta)^2]v^2, \tag{A10}$$

$$M_{s22}^2 = \mu_{s2}^2 + h_{a2}v_a^2 + \frac{1}{2}[f_2(\cos\beta)^2 + g_2(\sin\beta)^2]v^2, \tag{A11}$$

$$M_{s12}^2 = \frac{\mu v_a}{\sqrt{2}}. \tag{A12}$$

Notice that $h_{a1,a2}$ are chosen in the order of $(v/v_a)^2$ to ensure the electroweak scale m_{s1} and m_{s2}. For simplicity if we take the mixing terms M_{12}^2, M_{23}^2, and M_{13}^2 to be vanished, we obtain

$$\lambda_3 = -\lambda_4 - \frac{h_5 v_a^2}{\sin 2\beta v^2} \quad \text{and} \quad g_a = d_a = 0. \tag{A13}$$

Then λ_3 is also fixed once the values $\tan\beta$, h_5, and λ_4 are given, and at the moment $\sin\alpha = \sin\beta$. The trilinear couplings of SM Higgs H with charged scalars H^+, s_1, and s_2, respectively, are given by

$$\mu_{HH^+H^-} = \sin\beta[2\lambda_2(\cos\beta)^2 + \lambda_3(\sin\beta)^2 - \lambda_4(\cos\beta)^2]v,$$
$$\mu_{Hs_1^+s_1^-} = g_1 v\sin\beta, \qquad \mu_{Hs_2^+s_2^-} = g_2 v\sin\beta. \tag{A14}$$

As an illustration, taking $\tan\beta = 10$, $\lambda_1 = 0.5$, $\lambda_2 = 0.125$, $\lambda_4 = 0$, $\lambda_5 = -0.3$ as input values, then the related scalar masses are $m_h = 126$ GeV and $m_H \simeq m_A = m_{H^\pm} = 303$ GeV. On the other hand, for $\tan\beta = 50$, $\lambda_1 = \lambda_2 = 0.13$, $\lambda_4 = 0$, and $\lambda_5 = -0.1$, we have $m_H \simeq m_A = m_{H^\pm} = 389$ GeV. Both cases satisfy the experimental constraints [93]. In summary, having the scalar with a 126 GeV mass is insensitive to the value of h_5 due to the $\cos\beta$ suppression. The current constraint on the neutral scalar mass would give $|h_5(v_a^2/v^2)| \gtrsim 0.3$ for $\tan\beta = 10$ and $|h_5(v_a^2/v^2)| \gtrsim 0.06$ for $\tan\beta = 50$, by setting $\lambda_4 = 0$.

[1] G. 't Hooft, in *Recent Developments in Gauge Theories*, edited by G. 't Hooft *et al.* (Plenum, New York, 1980).
[2] R. D. Peccei and H. R. Quinn, Phys. Rev. Lett. **38**, 1440 (1977).
[3] R. D. Peccei and H. R. Quinn, Phys. Rev. D **16**, 1791 (1977).
[4] G. 't Hooft, Phys. Rev. Lett. **37**, 8 (1976); Phys. Rev. D **14**, 3432 (1976); **18**, 2199(E) (1978).
[5] R. Jackiw and C. Rebbi, Phys. Rev. Lett. **37**, 172 (1976).
[6] C. G. Callan, Jr., R. F. Dashen, and D. J. Gross, Phys. Lett. **63B**, 334 (1976).
[7] A. A. Belavin, A. M. Polyakov, A. S. Schwartz, and Y. S. Tyupkin, Phys. Lett. **59B**, 85 (1975).
[8] S. L. Adler, Phys. Rev. **177**, 2426 (1969).
[9] J. S. Bell and R. Jackiw, Nuovo Cimento A **60**, 47 (1969).
[10] V. Baluni, Phys. Rev. D **19**, 2227 (1979).
[11] R. J. Crewther, P. Di Vecchia, G. Veneziano, and E. Witten, Phys. Lett. **88B**, 123 (1979); **91B**, 487(E) (1980).
[12] P. Cea and G. Nardulli, Phys. Lett. **144B**, 115 (1984).
[13] H. J. Schnitzer, Phys. Lett. **139B**, 217 (1984).
[14] M. M. Musakhanov and Z. Z. Israilov, Phys. Lett. **137B**, 419 (1984).

[15] C. A. Baker, D. D. Doyle, P. Geltenbort, K. Green, M. G. D. van der Grinten, P. G. Harris, P. Iaydjiev, S. N. Ivanov *et al.*, Phys. Rev. Lett. **97**, 131801 (2006).
[16] S. Weinberg, Phys. Rev. Lett. **40**, 223 (1978).
[17] F. Wilczek, Phys. Rev. Lett. **40**, 279 (1978).
[18] C. Vafa and E. Witten, Phys. Rev. Lett. **53**, 535 (1984).
[19] R. D. Peccei, Lect. Notes Phys. **741**, 3 (2008).
[20] J. E. Kim, Phys. Rep. **150**, 1 (1987).
[21] H.-Y. Cheng, Phys. Rep. **158**, 1 (1988).
[22] J. Beringer *et al.* (Particle Data Group), Phys. Rev. D **86**, 010001 (2012).
[23] S. Andriamonje *et al.* (CAST Collaboration), J. Cosmol. Astropart. Phys. 04 (2007) 010.
[24] S. Aune *et al.* (CAST Collaboration), Phys. Rev. Lett. **107**, 261302 (2011).
[25] Y. Inoue, Y. Akimoto, R. Ohta, T. Mizumoto, A. Yamamoto, and M. Minowa, Phys. Lett. B **668**, 93 (2008).
[26] S. J. Asztalos, L. J. Rosenberg, K. van Bibber, P. Sikivie, and K. Zioutas, Annu. Rev. Nucl. Part. Sci. **56**, 293 (2006).
[27] S. J. Asztalos *et al.* (ADMX Collaboration), Phys. Rev. Lett. **104**, 041301 (2010).
[28] S. Weinberg, Phys. Rev. Lett. **43**, 1566 (1979).
[29] P.-H. Gu and H.-J. He, J. Cosmol. Astropart. Phys. 12 (2006) 010.
[30] P.-H. Gu and U. Sarkar, Phys. Rev. D **77**, 105031 (2008).
[31] P.-H. Gu, Nucl. Phys. **B872**, 38 (2013).
[32] A. Davidson and K. C. Wali, Phys. Rev. Lett. **60**, 1813 (1988).
[33] R. N. Mohapatra and G. Senjanovic, Z. Phys. C **17**, 53 (1983).
[34] Q. Shafi and F. W. Stecker, Phys. Rev. Lett. **53**, 1292 (1984).
[35] P. Langacker, R. D. Peccei, and T. Yanagida, Mod. Phys. Lett. A **01**, 541 (1986).
[36] M. Shin, Phys. Rev. Lett. **59**, 2515 (1987); **60**, 383(E) (1988).
[37] C. Q. Geng and J. N. Ng, Phys. Lett. B **211**, 111 (1988).
[38] X. G. He and R. R. Volkas, Phys. Lett. B **208**, 261 (1988); **218**, 508 (1989).
[39] C. Q. Geng and J. N. Ng, Phys. Rev. D **39**, 1449 (1989).
[40] E. Ma, Phys. Lett. B **514**, 330 (2001).
[41] S. Bertolini and A. Santamaria, Nucl. Phys. **B357**, 222 (1991).
[42] H. Arason, P. Ramond, and B. D. Wright, Phys. Rev. D **43**, 2337 (1991).
[43] M. Dine, W. Fischler, and M. Srednicki, Phys. Lett. **104B**, 199 (1981).
[44] A. R. Zhitnitsky, Yad. Fiz. **31**, 497 (1980) [Sov. J. Nucl. Phys. **31**, 260 (1980)].
[45] J. E. Kim, Phys. Rev. Lett. **43**, 103 (1979).
[46] M. A. Shifman, A. I. Vainshtein, and V. I. Zakharov, Nucl. Phys. **B166**, 493 (1980).
[47] L. M. Krauss and F. Wilczek, Phys. Rev. Lett. **62**, 1221 (1989).
[48] S. Nasri and S. Moussa, Mod. Phys. Lett. A **17**, 771 (2002).
[49] S. Kanemura, T. Nabeshima, and H. Sugiyama, Phys. Lett. B **703**, 66 (2011).
[50] C. D. Froggatt and H. B. Nielsen, Nucl. Phys. **B147**, 277 (1979).
[51] J. E. Kim, Phys. Rev. D **31**, 1733 (1985).
[52] K. Choi and J. E. Kim, Phys. Rev. D **32**, 1828 (1985).
[53] M. C. Gonzalez-Garcia, M. Maltoni, J. Salvado, and T. Schwetz, J. High Energy Phys. 12 (2012) 123.
[54] J. Adam *et al.* (MEG Collaboration), Phys. Rev. Lett. **107**, 171801 (2011).
[55] R. Kitano, M. Koike, and Y. Okada, Phys. Rev. D **66**, 096002 (2002); **76**, 059902(E) (2007).
[56] W. H. Bertl *et al.* (SINDRUM II Collaboration), Eur. Phys. J. C **47**, 337 (2006).
[57] A. Badertscher, K. Borer, G. Czapek, A. Fluckiger, H. Hanni, B. Hahn, E. Hugentobler, H. Kaspar *et al.*, Lett. Nuovo Cimento Soc. Ital. Fis. **28**, 401 (1980).
[58] A. Badertscher, K. Borer, G. Czapek, A. Fluckiger, H. Hanni, B. Hahn, E. Hugentobler, A. Markees *et al.*, Nucl. Phys. **A377**, 406 (1982).
[59] C. Dohmen *et al.* (SINDRUM II Collaboration), Phys. Lett. B **317**, 631 (1993).
[60] W. Honecker *et al.* (SINDRUM II Collaboration), Phys. Rev. Lett. **76**, 200 (1996).
[61] U. Bellgardt *et al.* (SINDRUM Collaboration), Nucl. Phys. **B299**, 1 (1988).
[62] G. W. Bennett *et al.* (Muon G-2 Collaboration), Phys. Rev. D **73**, 072003 (2006).
[63] J. Beringer *et al.* (Particle Data Group Collaboration), Phys. Rev. D **86**, 010001 (2012).
[64] G. C. Branco, P. M. Ferreira, L. Lavoura, M. N. Rebelo, M. Sher, and J. P. Silva, Phys. Rep. **516**, 1 (2012).
[65] W.-F. Chang, J. N. Ng, and J. M. S. Wu, Phys. Rev. D **86**, 033003 (2012).
[66] A. G. Beda, E. V. Demidova, A. S. Starostin, V. B. Brudanin, V. G. Egorov, D. V. Medvedev, M. V. Shirchenko, and T. Vylov, Phys. Part. Nucl. Lett. **7**, 406 (2010).
[67] K. Fujikawa and R. E. Shrock, Phys. Rev. Lett. **45**, 963 (1980).
[68] M. B. Voloshin, Yad. Fiz. **48**, 804 (1988) [Sov. J. Nucl. Phys. **48**, 512 (1988)].
[69] S. M. Barr, E. M. Freire, and A. Zee, Phys. Rev. Lett. **65**, 2626 (1990).
[70] N. F. Bell, V. Cirigliano, M. J. Ramsey-Musolf, P. Vogel, and M. B. Wise, Phys. Rev. Lett. **95**, 151802 (2005).
[71] P. Sikivie and Q. Yang, Phys. Rev. Lett. **103**, 111301 (2009).
[72] O. Erken, P. Sikivie, H. Tam, and Q. Yang, Phys. Rev. D **85**, 063520 (2012).
[73] P. Sikivie, Phys. Lett. B **432**, 139 (1998).
[74] P. Sikivie, Phys. Rev. D **60**, 063501 (1999).
[75] ATLAS Collaboration, Phys. Lett. B **716**, 1 (2012).
[76] S. Chatrchyan *et al.* (CMS Collaboration), Phys. Lett. B **716**, 30 (2012).
[77] ATLAS Collaboration, Report No. ATLAS-CONF-2013-034.
[78] Please see http://moriond.in2p3.fr/QCD/2013/qcd.html.
[79] G. Cacciapaglia, A. Deandrea, and J. Llodra-Perez, J. High Energy Phys. 06 (2009) 054.
[80] J. Cao, Z. Heng, T. Liu, and J. M. Yang, Phys. Lett. B **703**, 462 (2011).

[81] U. Ellwanger, J. High Energy Phys. 03 (2012) 044.
[82] V. Barger, M. Ishida, and W.-Y. Keung, Phys. Rev. Lett. **108**, 261801 (2012).
[83] A. Azatov, R. Contino, and J. Galloway, J. High Energy Phys. 04 (2012) 127.
[84] P. P. Giardino, K. Kannike, M. Raidal, and A. Strumia, J. High Energy Phys. 06 (2012) 117.
[85] M. Carena, I. Low, and C. E. M. Wagner, J. High Energy Phys. 08 (2012) 060.
[86] N. D. Christensen, T. Han, and S. Su, Phys. Rev. D **85**, 115018 (2012).
[87] M. Carena, S. Gori, N. R. Shah, C. E. M. Wagner, and L.-T. Wang, J. High Energy Phys. 07 (2012) 175.
[88] C.-W. Chiang and K. Yagyu, Phys. Rev. D **87**, 033003 (2013).
[89] C.-S. Chen, C.-Q. Geng, D. Huang, and L.-H. Tsai, Phys. Rev. D **87**, 075019 (2013).
[90] A. Djouadi, J. Kalinowski, and M. Spira, Comput. Phys. Commun. **108**, 56 (1998).
[91] ATLAS Collaboration, Report No. ATLAS-CONF-2012-158.
[92] J. Pumplin, D. R. Stump, J. Huston, H. L. Lai, P. M. Nadolsky, and W. K. Tung, J. High Energy Phys. 07 (2002) 012.
[93] O. Eberhardt, U. Nierste, and M. Wiebusch, J. High Energy Phys. 07 (2013) 118.